Assessing Downscaling Techniques for Frequency Analysis, Total Precipitation and Rainy Days Estimation in CMIP6 Simulations over Hydrological Years

David A. Jimenez[1], Andrea Menapace[2], Ariele Zanfei[3] , Eber José de Andrade[1,4], Bruno Brentan[1]

[1]Hydraulic and Water Resources Department, Federal University of Minas Gerais UFMG, 31270-901, MG, Brazil
[2]Faculty of Science and Technologies, Free University of Bozen-Bolzano, 39100 Bolzano, Italy
[3]AIAQUA S.r.l., Via Volta 13/A, Bolzano, Italy.
[4]The Geological Survey of Brazil, 30140-002, MG, Brazil

Correspondence to: David A. Jimenez O. (dajimenezoo30@gmail.com)

Abstract. General circulation models generate climate simulations on grids with resolutions ranging from 50 km to 600 km. The resulting coarse spatial resolution of the model outcomes requires post-processing routines to ensure reliable climate information for practical studies, prompting the widespread application of downscaling techniques. However, assessing the effectiveness of multiple downscaling techniques is essential, as their accuracy varies depending on the objectives of the analysis and the characteristics of the case study. In this context, this study aims to evaluate the performance of downscaling the daily precipitation series in the Metropolitan Region of Belo Horizonte, Brazil, with the final scope of performing frequency analyses, and estimating total precipitation and the number of rainy days per hydrological year at both annual and multiannual levels. To develop this study, 78 climate models with a horizontal resolution of 100 km, which participated in the SSP1-2.6 and/or SSP5-8.5 scenarios of CMIP6, are employed. The results highlight that adjusting the simulations from the general circulation models by Delta Method, Quantile Mapping, and Regression Trees produces accurate results for estimating the total precipitation and number of rainy days. Finally, it is noted that employing downscaled precipitation series through Quantile Mapping and Regression Trees yields promising results also in terms of the frequency analyses.

1 Introduction

As emphasised by the Intergovernmental Panel on Climate Change (IPCC), Global Climate Models (GCMs) represent the most advanced climate simulation tools and play a fundamental role in evaluating future climate scenarios (IPCC, 2014). GCMs have the capability to generate coherent climate estimations both physically and geographically. The GCMs are used to examine the effect of increasing greenhouse gas emissions on climatic variables (Ostad-Ali-Askari et al., 2020). However, due to their low spatial resolution (50-600 km), they are unable to adequately reproduce the climatic variables of small areas such as basins and sub-basins (Ozbuldu & Irvem, 2021), whereby the application of downscaling techniques has become a standard procedure (Worku et al., 2021; Olsson et al., 2016).

Downscaling aims to refine low-resolution global climate projections to local or regional scales by identifying relationships between observed climate data and simulations from GCMs (Jimenez, 2022; Zhang & Li, 2020). Downscaling enhances the representativeness of projected climate conditions, making them more accurate of local climate conditions. Ensuring adequate downscaling is essential since adjusted series are employed to assess the impacts of climate change on regional scales (Teutschbein et al., 2011). If an inadequate methodology of downscaling is selected for future climate projections, misinterpretation and inaccurate estimation of the effects of climate change, with detrimental consequences for long-term planning in the management of climate change impacts could be done (Rastogi et al., 2022). For instance, underestimating regional-scale responses to climate change can result in a lack of preparedness from a planning and mitigation perspective. Conversely, overestimating these responses can lead to an excessive budget allocation for addressing the consequences.

Given the variety of downscaling techniques available in the literature (Delta Method, Quantile Mapping, Machine Learning Techniques, etc.), Rastogi et al. (2022), Yang et al. (2019), and Onyutha et al. (2016) report that the efficiency of downscaling techniques varies depending on several reasons, such as the research objectives, the data and the case study, making it necessary to evaluate multiple techniques in each specific study. The analysis and characterization of changes in precipitation patterns is one of the most relevant thematic areas in research addressing the impacts of climate change. Mahla et al. (2019), Salehnia et al. (2019), Yang et al. (2019), Sachindra et al. (2018) and Hashmi et al. (2011), evaluated the performance of downscaled techniques to reduce precipitation.

Mahla et al. (2019) indicated that downscaling monthly precipitation based on multiple linear regressions showed promising results for the study area. On the other hand, Salehnia et al. (2019) identified that Dynamic Downscaling (DDS) provides better results than Statistical Downscaling (SDS) in total annual and seasonal precipitation downscaling, pointing out that SDS is computationally simpler than DDS. Conversely, Yang et al., (2019), found that methods based on quantile mapping demonstrate better performance in the downscaling of seasonal scale and extreme precipitation Compared to the function transform method (CDF-t). Sachindra et al. (2018) recommended using a Regional Vector Machine (RVM) over Genetic Programming (GP), Artificial Neural Networks (ANNs) and Support Vector Machine (SVM) for monthly precipitation downscaling. Finally, Hashmi et al. (2011) identified that the GP provides better results for daily precipitation downscaling than ANNs.

Most of the studies have focused on assessing the efficiency of downscaling techniques for monthly, annual, and seasonal precipitation by the civil year (Kreienkamp et al., 2019; Ozbuldu & Irvem, 2021). However, only a few studies have been conducted for the hydrological year. Instead, no studies were identified evaluating the effectiveness of these techniques for conducting frequency analysis.

Tabari et al. (2021), Liu et al. (2020), Norris et al. (2020) and Hassanzadeh et. al. (2014) indicated that climate change could transform or modify temperature and relative humidity patterns, leading to the intensification of extreme weather events (Roca

et al., 2019). Thus, authors such as Fadhel et al., (2017), Shahabul and Elshorbagy (2015) and Waters et al., (2003) emphasize that in the current context of climate change, it is necessary to identify potential changes in Intensity-Duration-Frequency (IDF) relationships.

Therefore, it is essential to assess the representativeness of downscaling techniques for conducting frequency analyses, because the number of studies evaluating the alterations in IDF relationships in the climate change context from simulations of GCMs has been increasing (e.g., Ghasemi Tousi et al. (2021), Hassanzadeh et al. (2014) and Hashmi et al. (2011)). The assessment of changes in IDF relationships in climate change scenarios plays a fundamental role in decision-making related to the planning of hydraulic infrastructure, drainage systems, flood prevention, and water resource management. Identifying these changes enables authorities, engineers, and planners to incorporate the new climate realities into the development of infrastructure projects.

To ensure accurate downscaling and enable a correct estimation and interpretation of the impacts of climate change on IDF relationships, the proposed work aims to investigate the performance of some of the most recognized downscaling techniques in the literature, such as the Delta Method (DM), Quantile Mapping (QM), and Regression Trees (RT), in terms of frequency analysis. Additionally, the techniques were also evaluated for their ability to reproduce total precipitation and the number of rainy days per hydrological year and at a multiyear level.

In this way, the present study contributes to the identification and selection of downscaling techniques that can be applied in research that assessing changes in IDF relationships from CMIP6 projections, as well as in studies evaluating changes in the number of rainy days and total precipitation at the multiyear level in the context of climate change. In order to facilitate the paper's understanding, the second section presents the study area, the data used, the downscaling techniques considered, and the efficiency metrics used to evaluate the downscaling techniques. The third section presents the results and discussion, while the fourth section draws the conclusions and final considerations.

2. Data and Methodology

2.1 Study Area and historical rainfall records

The study was conducted in the Metropolitan Region of Belo Horizonte (MRBH), which is located between latitudes 18.0º and 20.5º south and longitudes 43.15º and 44.75º east, in the central region of the state of Minas Gerais, Brazil. The MRBH covers an area of 9468 km^2 with a hydrological year starting in October, with precipitation occurring from October to March. Monthly precipitation can exceed 300 mm/month. The MRBH monitoring network comprises more than 120 pluviometric stations distributed throughout the region (see Figure 1a).

The MRBH is selected because, as Nunes (2018) indicated, a significant portion of MRBH is directly or indirectly experiencing the consequences of extreme rainfall events. Between 1928 and 2000, 200 floods were recorded in Belo Horizonte, with 69.5% of these events occurring in the last two decades analysed. Furthermore, over 37 flood events were reported between 2000 and 2020.

The rainfall records for the MRBH are obtained from the Hydrological Information System (Hidroweb) of the Brazilian National Water Agency, available at https://www.snirh.gov.br/hidroweb/serieshistoricas. Upon downloading the rainfall data, we ensured its consistency by constructing double mass curves using total precipitation data for each hydrological year. Rainfall stations with over 30 years of consistent records and with missing data below 10% were selected. It is important to note that we did not fill in any missing data, as this could introduce uncertainties in the results.

Double mass curves are processed to perform consistency analysis on the collected data. Stations with distances less than 44 km and a correlation equal to or greater than 0.7 from each reference station were selected to perform this calculation. It was evident that only 29 stations have more than 30 years of consistent records and missing data below 10%. Thus, the study was developed from the rainfall information of the 29 stations shown in Figure 1b.
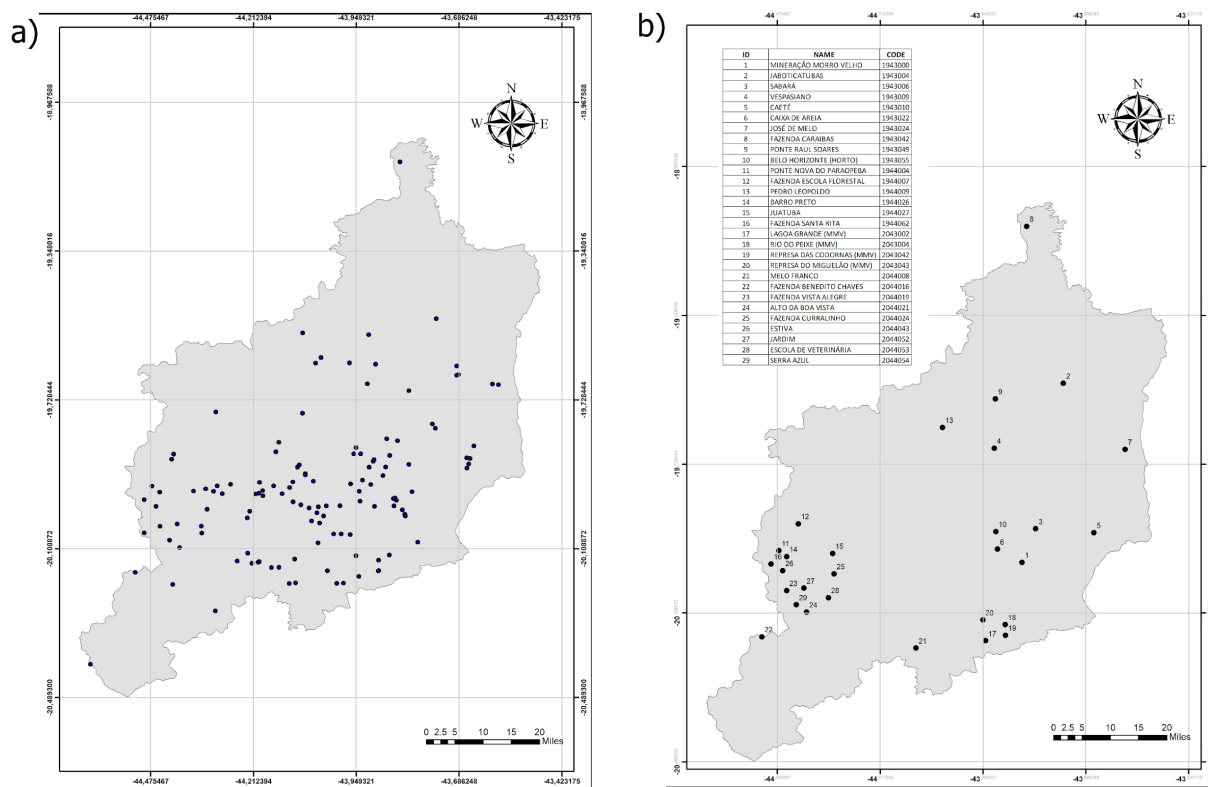
Figure 1 Pluviometric stations of MRBH: a) monitoring network of pluviometric stations and b) selected pluviometric stations used in the present study.

2.2 Simulation of rainfall conditions

The daily precipitation data simulated for the historical period (1850-2014) by GCMs with the resolution of 100 km, participating in emission scenarios SSP1-2.6 and/or SSP5-8.5 of CMIP6, were obtained from https://esgf-node.llnl.gov/search/cmip6/. It is important to emphasize that all available simulations with a resolution of 100 km have been included to consider all the ensembles available for each climate model. This choice was made with the intention of utilizing all available model outputs and thus providing a more robust analysis.

The SSP5-8.5 and SSP1-2.6 scenarios are selected as the CMIP6 scenarios that project the highest and lowest temperature increases respectively. In the case of SSP5-8.5 scenario, it is assumed that the economic and social development of humankind until the end of the 21st century will be governed by: i) high exploitation of resources, ii) intensive use of fossil fuels, iii) high global energy demand. All these factors lead to high greenhouse gas concentrations, resulting in a radiative forcing of 8.5 W m-2 by the end of the 21st century (Riahi et al., 2016). On the other hand, SSP1-2.6 scenario considers that: i) the world is turning towards sustainability, ii) there is a commitment by nations to reduce social inequalities, iii) consumption is oriented towards low material growth and low resource and energy consumption. All these factors were combined with a radiative forcing of 2.6 W m^{-2} (Riahi et al., 2016). The simulations contemplated are presented in Table 1.

Table 1 Overview of the CMIP6 GCM ensemble used in this study (r –realisation or ensemble member; i –initialisation method; p–physics; f –forcing).

ID	Model	Ensamble	SSP1-2.6 future	SSP5-8.5 future
1	CESM2	r11i1f1p1	X	✓
2	CESM2	r4i1f1p1	✓	X
3	CESM2-WACCM	r1i1f1p1	X	✓
4	CESM2-WACCM	r2i1f1p1	X	X
5	CESM2-WACCM	r3i1f1p1	X	✓
6	CMCC-CM2-SR5	r1i1f1p1	✓	✓
7	CMCC-ESM2	r1i1f1p1	✓	✓
8	EC-Earth3-CC	r1i1f1p1	X	✓
9	EC-Earth3	r101i1p1f1	✓	✓
10	EC-Earth3	r102i1p1f1	✓	✓
11	EC-Earth3	r103i1p1f1	✓	✓
12	EC-Earth3	r104i1p1f1	✓	✓
13	EC-Earth3	r105i1p1f1	✓	✓
14	EC-Earth3	r106i1p1f1	✓	✓
15	EC-Earth3	r107i1p1f1	✓	✓
16	EC-Earth3	r108i1p1f1	✓	✓
17	EC-Earth3	r109i1p1f1	✓	✓
18	EC-Earth3	r110i1p1f1	✓	✓
19	EC-Earth3	r111i1p1f1	✓	✓
20	EC-Earth3	r112i1p1f1	✓	✓
21	EC-Earth3	r113i1p1f1	✓	✓
22	EC-Earth3	r114i1p1f1	✓	✓
23	EC-Earth3	r115i1p1f1	✓	✓
24	EC-Earth3	r116i1p1f1	✓	✓
25	EC-Earth3	r117i1p1f1	✓	✓
26	EC-Earth3	r118i1p1f1	✓	✓
27	EC-Earth3	r119i1p1f1	✓	✓
28	EC-Earth3	r11i1f1p1	✓	✓
29	EC-Earth3	r121i1p1f1	✓	✓
30	EC-Earth3	r122i1p1f1	✓	✓
31	EC-Earth3	r123i1p1f1	✓	✓
32	EC-Earth3	r124i1p1f1	✓	✓

ID	Model	Ensamble	SSP1-2.6 future	SSP5-8.5 future		ID	Model	Ensamble	SSP1-2.6 future	SSP5-8.5 future
33	EC-Earth3	r125i1p1f1	✓	✓		56	EC-Earth3	r147i1p1f1	✓	✓
34	EC-Earth3	r126i1p1f1	✓	✓		57	EC-Earth3	r148i1p1f1	✓	✓
35	EC-Earth3	r127i1p1f1	✓	✓		58	EC-Earth3	r149i1p1f1	✓	✓
36	EC-Earth3	r128i1p1f1	✓	✓		59	EC-Earth3	r150i1p1f1	✓	✓
37	EC-Earth3	r129i1p1f1	✓	✓		60	EC-Earth3	r15i1p1f1	✓	✓
38	EC-Earth3	r130i1p1f1	✓	✓		61	EC-Earth3	r1i1f1p1	✓	✓
39	EC-Earth3	r131i1p1f1	✓	✓		62	EC-Earth3	r3i1f1p1	X	✓
40	EC-Earth3	r132i1p1f1	✓	✓		63	EC-Earth3	r4i1f1p1	✓	✓
41	EC-Earth3	r133i1p1f1	✓	✓		64	EC-Earth3	r6i1f1p1	✓	✓
42	EC-Earth3	r134i1p1f1	✓	✓		65	EC-Earth3-Veg	r1i1f1p1	✓	✓
43	EC-Earth3	r135i1p1f1	✓	✓		66	EC-Earth3-Veg	r2i1f1p1	X	✓
44	EC-Earth3	r136i1p1f1	✓	✓		67	EC-Earth3-Veg	r3i1f1p1	✓	✓
45	EC-Earth3	r137i1p1f1	✓	✓		68	EC-Earth3-Veg	r4i1f1p1	✓	✓
46	EC-Earth3	r138i1p1f1	✓	✓		69	EC-Earth3-Veg	r6i1f1p1	✓	✓
47	EC-Earth3	r139i1p1f1	✓	✓		70	GFDL-CM4	r1i1f1p1	X	✓
48	EC-Earth3	r13i1p1f1	✓	✓		71	GFDL-ESM4	r1i1f1p1	✓	✓
49	EC-Earth3	r140i1p1f1	✓	✓		72	INM-CM4-8	r1i1f1p1	✓	✓
50	EC-Earth3	r141i1p1f1	✓	✓		73	INM-CM5-0	r1i1f1p1	✓	✓
51	EC-Earth3	r142i1p1f1	✓	✓		74	MPI-ESM1-2-HR	r1i1f1p1	✓	✓
52	EC-Earth3	r143i1p1f1	✓	✓		75	MPI-ESM1-2-HR	r2i1f1p1	✓	✓
53	EC-Earth3	r144i1p1f1	✓	✓		76	MRI-ESM2-0	r1i1f1p1	✓	✓
54	EC-Earth3	r145i1p1f1	✓	✓		77	NorESM2-MM	r1i1f1p1	✓	✓
55	EC-Earth3	r146i1p1f1	✓	✓		78	TaiESM1-R1	r1i1f1p1	✓	✓

124

2.3 Downscaling

The primary approaches to downscaling are SDS and DDS. In this study, two of the most popular SDS techniques were evaluated: the Delta Method, Quantile Mapping, as well as the ML-Method Regression Trees. Due to their simplicity and low computational effort, DM and QM have been widely used in many research studies. In the case of DM, the investigations developed by Salehnia et al., (2020), Salehnia et al., (2019) and Teutschbein & Seibert (2012) are noteworthy. The study developed by Salehnia et al., (2020) aims to investigate the impact of climate change on rainfed wheat yield in the Khorasan-e Razavi province of northeast Iran. The study used climate projections from GCMs to assess the potential impact of climate changes on rainfed wheat yield over the next decades (2019–2038). The DM was used to correct the simulations of temperature and precipitation on the daily and monthly scales. On the other hand, Salehnia et al., (2019), compared the performance of DM and DDS in terms of the amount and number of wet days, and total precipitation at annual and seasonal scales. The results showed that DDS has better performance than DM. Similarly, it is highlighted that DM underestimates the annual mean

precipitation and the number of wet days, while DDS overestimates them. Finally, Teutschbein & Seibert (2012) compared the performance of different downscaling techniques to correct precipitation and temperature. Their results highlighted that the Delta Method is a stable and robust method, with the ability to produce future time series with dynamics similar to current conditions. However, the method does not consider potential changes in future climatic dynamics.

With respect to QM, the studies conducted by Enayati et al. (2021), Heo et al. (2019), and Jakob Themeßl et al. (2011) are noteworthy. In the study conducted by Enayati et al. (2021), the capability of bias correction in precipitation and temperature simulations of GCMs using QM technique was evaluated. The results indicated that non-parametric methods of Quantile Mapping exhibited the best performance. On the other hand, Heo *et al.* (2019), evaluated the use of different probability distributions in QM, and the results showed that the selection of the probability distribution could lead to better or worse results. Finally, Jakob Themeßl et al. (2011) indicated that the use of quantile mapping has better performance in the estimation of high quantiles. In this way, the use of this technique could present an advantage in the case of extreme precipitation events.

In the case of RT, the studies conducted by Khalid and Sitanggang (2022) and Hutengs and Vohland (2016) stand out. Khalid and Sitanggang (2022) compared various ML methods for downscaling precipitation, yielding that RT performed best. On the other hand, the study conducted by Hutengs and Vohland (2016) adopted RT to enhance the spatial resolution of temperature based on land surface temperature and reflectance with favourable results.

A Pixel-Station downscaling approach was developed. Observational data from each station were collected along with simulated GCM data, extracted from the pixel containing that station. For all the selected pairs of time series, the temporal consistency between daily precipitation observed and simulated was guaranteed by selecting the simulated data only for the day in which the observation data are presented. Once the simulated series was obtained, the evaluated downscaling techniques were applied for each selected point.

2.3.1 Delta Method

In this method, differences or 'deltas' between observed and GCM-simulated climatic conditions in the historical period are calculated. Subsequently, assuming that these differences or deltas remain constant over time, they are applied to GCMs-simulated future climate projections, thus refining climate projections at local or regional levels. The mathematical equation employed by the Delta method is presented below:

$$P_{SD}^{Delta} = P_{Mod,daily} \left(\frac{P_{obs}}{\underline{P_{Mod}}} \right)_{Monthly} \tag{2}$$

162 Where: P_{SD}^{Delta} represents the downscaled precipitation, $P_{Mod,daily}$ represents the simulated precipitation by the GCMs, $\underline{P}_{obs}$

163 represents the average monthly precipitation of the station and $\underline{P}_{Mod}$ represents the average monthly precipitation simulated

164 by GCMs.

2.3.2 Quantile Mapping

166 QM is based on the principle of matching the quantiles of observed and GCMs-simulated distributions. The process begins

167 with estimating the quantiles of the observed series. Then, for the future period, the empirical probability associated with the

168 quantile simulated by the GCMs is estimated. This probability is used in the inverse probability function of observed quantiles,

169 thus obtaining the downscaled value. The following is a mathematical description of the method of precipitation:

$$P_{SD}^{QQ} = F_o^{-1}[F_M(P_M)] \tag{1}$$

170

171 where P_{SD}^{QQ} is the precipitation with *downscaling*, F_o^{-1} is the inverse empirical probability function of daily precipitation for

172 the historic period, F_M is the empirical probability function of simulated precipitation, and P_M is the simulated precipitation by

173 MCGs.

2.3.3 Regression Trees

175 Regression Trees are a Machine-Learning technique used to build predictive models. These models are created by recursively

176 dividing the sample space and adjusting predictive models for each subdivision (Loh, 2011). The main goal of this technique

177 is to partition the sample space into k units and create a predictive model for each subspace. This approach enables the

178 prediction of the variable of interest, Y, using a piecewise function of the type:

$$Y = \{f_{E_0}(x), \quad x \in E_0 \ f_{E_1}(x), \quad x \in E_1 \ ... \ f_{E_k}(x), \\ x \in E_k \tag{3}$$

179

180 Where: Y is the predicted variable, $f_{E_i}(x)$ is the predictive model of the sample subspace E_i, and x is the predictor variable.

181 Downscaling using RT can incorporate more than one predictor variable to estimate the variable of interest, for example,

182 precipitation could be estimated using multiple variables simulated by General Circulation Models, such as temperature,

183 atmospheric pressure, and precipitation. However, it's important to note that the uncertainties in downscaling tend to increase

184 with the number of predictors. In this way, only daily precipitation is simulated as the predictor variable to minimize these

185 uncertainties.

186   The downscaling process was carried out using observed and simulated precipitation quantiles. This approach is used due to

187   the absence of a consistent temporal correlation between the observed and simulated rainfall magnitudes. Often, the simulated

188   precipitation by the GCMs did not match with the historical records, leading to instances where GCMs projected rainfall on

189   days when historical data indicated dry weather conditions. In the training stage, 85% of the records were used, while in the

190   validation stage, 15% were employed. The optimization of hyperparameters (Maximum number of splits, Split criterion) was

191   conducted using the automatic hyperparameter optimization function available in the 'fitrtree' function in Matlab.

2.4 Frequency Analysis

193   The frequency analysis is carried out using the maximum annual precipitation series, estimated from both historical records

194   and downscaling results. Initially, the stationarity and homogeneity of the maximum series are confirmed using the Spearman

195   (NERC, 1975) and Mann-Whitney (1947) statistical tests. These tests are applied at a 5% significance level, as specified by

196   Naghettini and Pinto (2007).

197   The frequency analysis is exclusively conducted on the series that exhibited homogeneity and stationarity. This analysis

198   considered various probability distributions, including Exponential, Gamma, Gumbel, GEV, Log-Normal, Pearson III, and

199   Log-Pearson III. The parameters for these distributions are estimated using L-moments method (Hosking, 1997). To evaluate

200   the adherence of the series to these probability distributions, the nonparametric Kolmogorov-Smirnov test is applied at a

201   significance level of 5%. For each station, the quantiles of precipitation associated with return periods of 2, 5, 10, 15, 30, 35,

202   45, 50, 60, 70, 80, 90, and 100 years were estimated based on the distribution that exhibited the best fit.

2.5 Comparison between estimates made with historical series and downscaling.

204   The efficiency of downscaling techniques was assessed in terms of total precipitation (TP) and the number of rainy days (RD)

205   at both the hydrological year and multiyear level. In the latter case, the total precipitation and rainy days are aggregated over

206   the available record period. Similarly, the techniques are examined in terms of frequency analysis.

207   The TP and RD by the hydrological year are evaluated using the Nash-Sutcliffe (NSE), Kling-Gupta (KGE), root-mean-square

208   error (RMSE), and the Pearson correlation coefficient (R). In the case of the multiyear level, the evaluation was performed

209   using the percentage error.

210   Nash-Sutcliffe (1979) and Gupta et al. (2009) indicated that NSE and KGE values of 1 represent an ideal match between

211   observed and simulated data. In the case of RMSE, a value of 0 signifies a perfect fit. Moreover, the R value, which falls

212   between 0 and 1, indicates a positive correlation. Values between -1 and 0 suggest a negative correlation, while those near 0

213   imply no correlation. Finally, a percentage error value of 0 indicates a perfect fit between observed and simulated data. The

214   equations used to calculate NSE, KGE, RMSE, R and percentage error are provided below:

$$NSE = 1 - \frac{\sum_{i=1}^{n}(X_i - X_i')^2}{\sum_{i=1}^{n}(X_i - \bar{X}_i)^2} \tag{4}$$

$$KGE = 1 - \sqrt{(r-1)^2 + \left(\frac{\sigma_i'}{\sigma_i} - 1\right)^2 + \left(\frac{\underline{X_i'}}{\underline{X_i}} - 1\right)^2} \tag{5}$$

$$RMSE = \sqrt{\frac{\sum_{i=1}^{n}(X_i - X_i')^2}{n}} \tag{6}$$

$$R = \frac{n(\sum X_i X_i') - (\sum X_i * \sum X_i')}{\sqrt{\left[n(\sum X_i^2) - (\sum X_i)^2\right] * \left[n(\sum X_i'^2) - (\sum X_i')^2\right]}} \tag{7}$$

$$\% \, Error = \frac{|X_i' - X_i|}{X_i} * 100 \tag{8}$$

215 Where X_i and X_i' are the observed and simulated values, while $\underline{X_i}$ and $\underline{X_i'}$ the mean of the observed and simulated values,

216 respectively. n represents the number of simulated data, σ_i' the standard deviation of the simulated values, σ_i the standard

217 deviation of the observed records, and R the correlation coefficient between the observed and simulated records.

3. Results and discussions

3.1 Total precipitation and number of rainy days per hydrological year

220 78 analyses were conducted both for total precipitation for the hydrological year and the number of rainy days, the median

221 values of NSE, KGE, RMSE, and R were computed to facilitate the analysis and interpretation of the results, emphasizing that

222 the median was chosen because it is less susceptible to extreme events.

Number of Rainy Days per hydrological year

224 Estimating the number of rainy days in the hydrological year, from downscaled series using DM, QM, and RT methods yields

225 unsatisfactory results in all evaluated models. Thus, Figure 2 and Table 2 reveal discrepancies in the number of rainy days

226 estimated per hydrological year from the downscaled series compared to observations. Without the application of any

227 downscaling technique (WDS), this difference is approximately 78 days. However, when using DM, QM, and RT as

228 downscaling techniques, the difference decreases to 73, 18, and 19 days, respectively. Thus, QM and RT stand out for providing

229 the greatest reduction in the discrepancy between the number of rainy days per hydrological year estimated from the

230 downscaled series compared to observations. Nonetheless, as mentioned and observed in Table 2 and Figure 2, the low NSE,

231 KGE, and R scores show that the estimation of the number of rainy days at the annual scale does not work well.

232

233
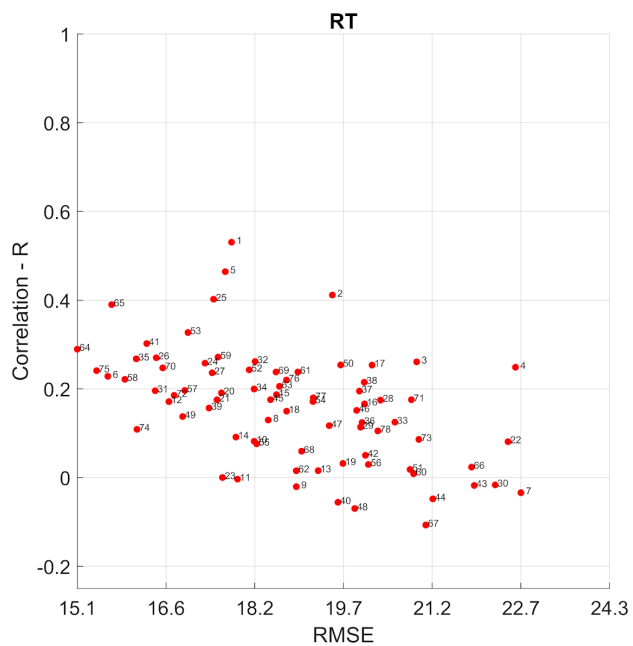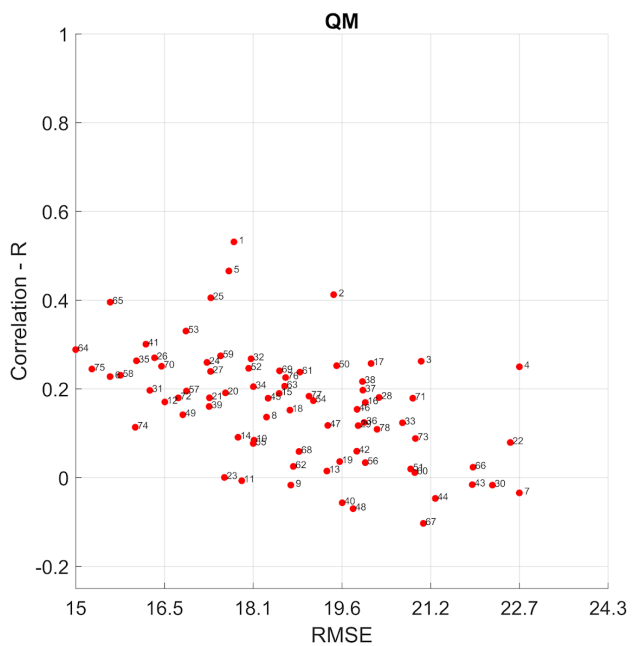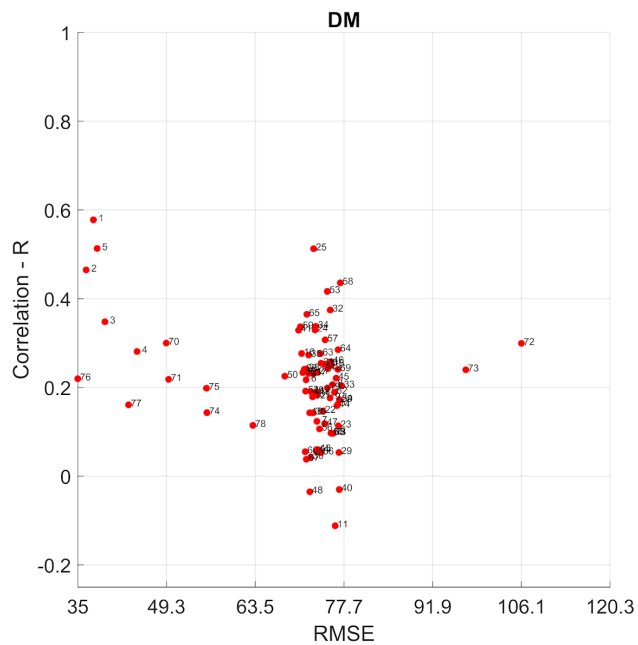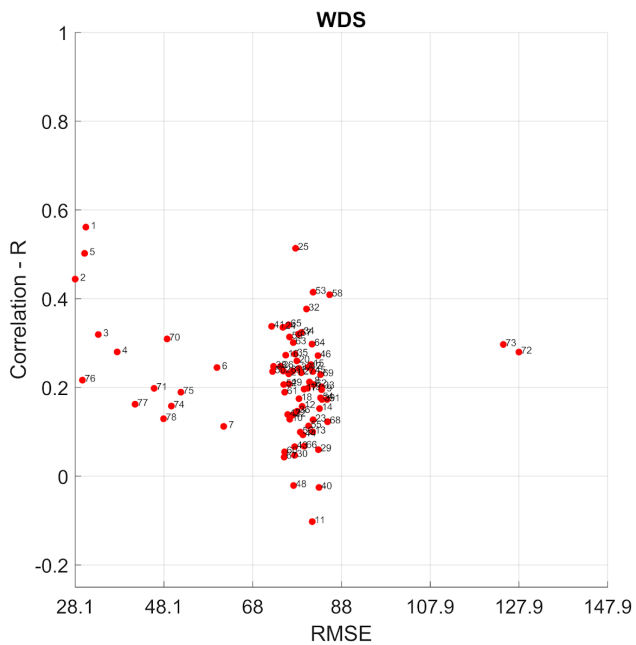
Figure 2 Median performance metrics (RMSE and R) for the estimated number of rainy days from precipitation series simulated by GCMs, without the application of downscaling techniques (WDS), as well as adjusted series obtained using the DM, QM, and RT.

237 Table 2 Summary of performance metrics for estimating the number of rainy days from without downscaling and reduced
238 series using DM, QM, and RT methods.

	WDS			DM			QM			RT		
	NSE	RMSE	KGE	NSE	RMSE	KGE	NSE	RMSE	KGE	NSE	RMSE	KGE
Maximum	-2.3	128	0.3	-4.5	106	0.2	-0.28	23	0.44	-0.29	23	0.44
Median	-44.2	78	-0.4	-39.0	73	-0.4	-1.46	18	0.05	-1.48	19	0.05
Minimum	-117.6	28	-0.8	-81.4	35	-0.7	-2.85	15	-0.21	-2.83	15	-0.20

239

240 As shown in Figure 3, the low performance of NSE, KGE observed in the Table 2 in the estimation of number of rainy days
241 per hydrological year, is associated with underestimations or overestimations.

242 As observed in Figure 3, an underestimation of the number of rainy days occurs when no downscaling techniques are applied.
243 This underestimation trend persists when the DM is applied, consistent with the results found by Salehnia et al., (2019).
244 However, when using QM and RT, this trend reverses, resulting in overestimation. The persistence of underestimation when
245 DM is applied may be related to the method of applying a constant correction factor per month. On the other hand, the shift
246 from underestimation to overestimation when using QM and RT can be attributed to the relationship between simulated and
247 observed quantiles. Therefore, it is possible that there is a reclassification of dry days (P <= 1.0 mm) as wet days (P>1.0 mm)
248 (i.e., a simulated quantile of 0.2 mm can be associated with observed precipitation >1 mm).

249 The median percentage underestimation errors were 85.21%, 79.3%, 14.50%, and 13.70% for WDS, DM, QM, and RT,
250 respectively. Meanwhile, the average overestimations were 12.54% and 13.78% for QM and RT, respectively.
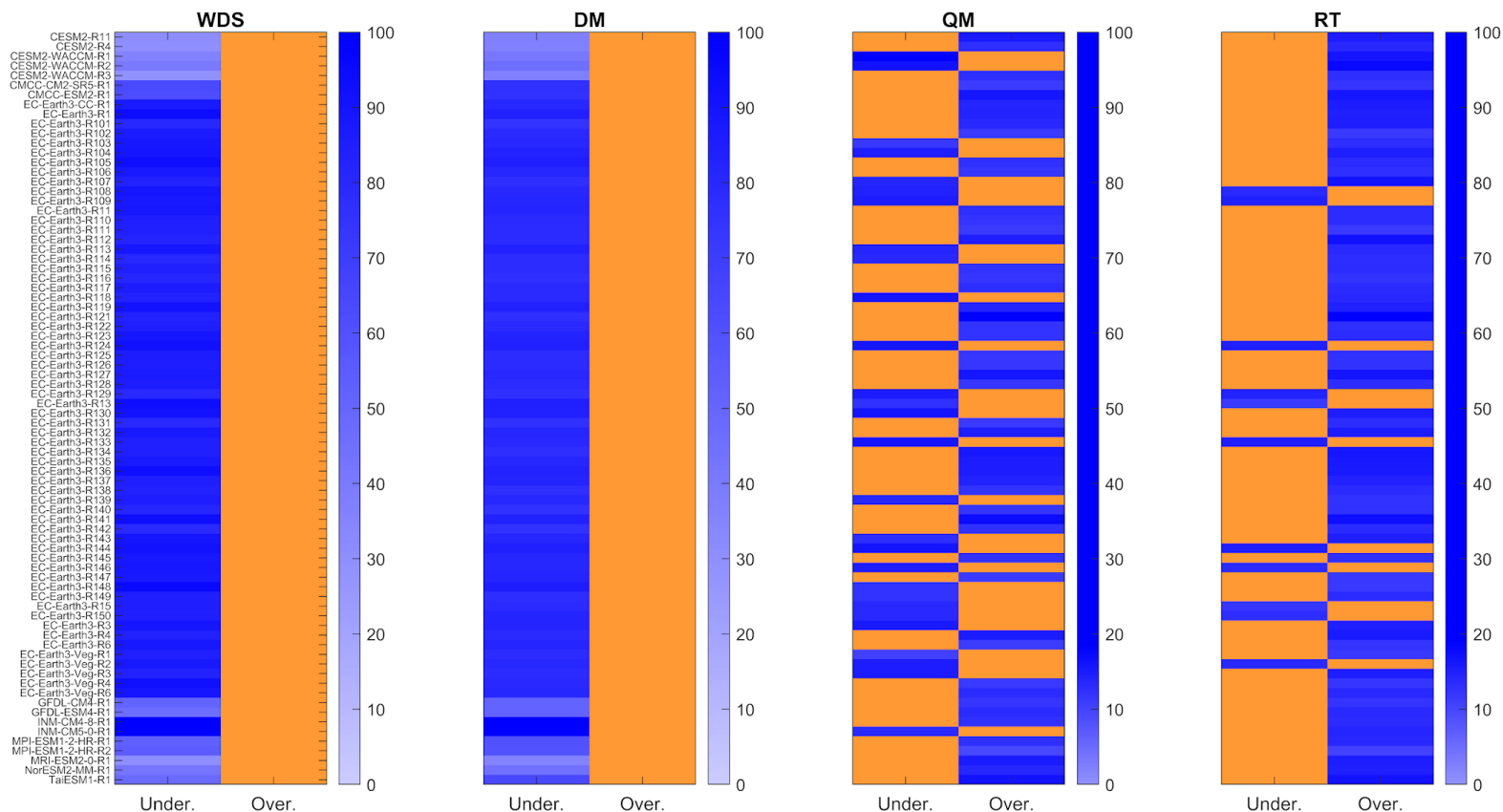
Figure 3 Median percentage error of underestimation or overestimation of total number of rainy days per hydrological year. The percentage error of the prevailing condition of underestimation (Under.) or overestimation (Over.) is represented in blue, while the non-prevailing condition is depicted in orange. For example, if underestimation is prevalent, overestimation is represented in orange. WDS represents the condition without the application of downscaling techniques, DM corresponds to the condition when Delta Method is applied, QM represents the condition when Quantile Mapping is applied, and RT indicates the condition of applying Regression Trees as a downscaling technique.

Total precipitation per hydrological year

Estimating the total precipitation per hydrological year from the downscaled series obtained through the application of DM, QM, and RT does not guarantee good results. Thus, when no downscaling technique is applied, the difference between the total precipitation estimated from the downscaled series differs, on median 413.84 mm. In the case where DM is applied, this difference decreases to approximately 361.42 mm. However, when QM and RT are applied, the differences are higher than when no downscaling technique is applied, with median differences of 433.10 mm and 434.64 mm, respectively (see Figure 4). That way, the difference between the total precipitation estimated from the downscaled series by QM and RT increases by approximately 4% compared to the estimations when no downscaling technique is applied and decreases by 12% when the DM is applied.

On the other hand, the low NSE, KGE, and R scores, as shown in Figure 4, indicate that the estimation of total precipitation at the annual scale from the downscaled series does not perform well.

Table 3 Summary of performance metrics for estimating the total precipitation by hydrological year without downscaling (WDS) and with DM, QM, and RT methods.

	WDS			DM			QM			RT		
	NSE	RMSE	KGE	NSE	RMSE	KGE	NSE	RMSE	KGE	NSE	RMSE	KGE
Maximum	-0.53	654.02	0.36	-0.09	482.54	0.38	-0.66	524.55	0.31	-0.67	526.83	0.31
Median	-1.43	413.84	0.07	-0.77	361.42	0.08	-1.58	433.10	0.00	-1.59	434.64	-0.01
Minimum	-5.14	324.65	-0.21	-1.75	277.78	-0.24	-2.79	343.72	-0.29	-2.81	344.30	-0.29

In the same way as with the number of rainy days, the difference between the total precipitation per hydrological year estimated from observed data and downscaled data is associated with underestimations and overestimations. When no downscaling technique is applied, an underestimation of total precipitation per hydrological year is observed. However, when DM, QM, or RT is applied, this underestimation changes to overestimation (see Figure 5).

In the case of QM and RT, the overestimation of total hydrological precipitation per year (Figure 4) is related to the overestimation of the number of rainy days (Figure 3) most of the time. Thus, it is noticeable that the application of QM and RT increases both the number of rainy days in the hydrological year and the magnitudes of simulated precipitations. However, this trend is intrinsic to the conceptual foundation of these methods. For example, during the application of QM or RT, a simulated quantile of 1 mm of rain can be associated with an observed quantile of 20 mm of rain.

The median percentage underestimation errors were 25.58%, 17,02%, 18.74%, and 18.77% for WDS, DM, QM, and RT, respectively. Meanwhile, the average overestimations were 22.37%, 14.63%, 18.37%, and 18.30% for WDS, DM, QM, and RT, respectively.

284
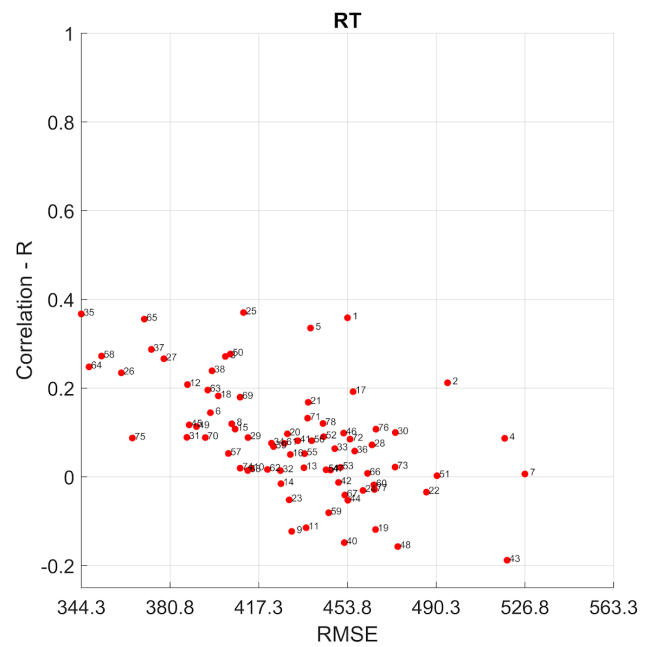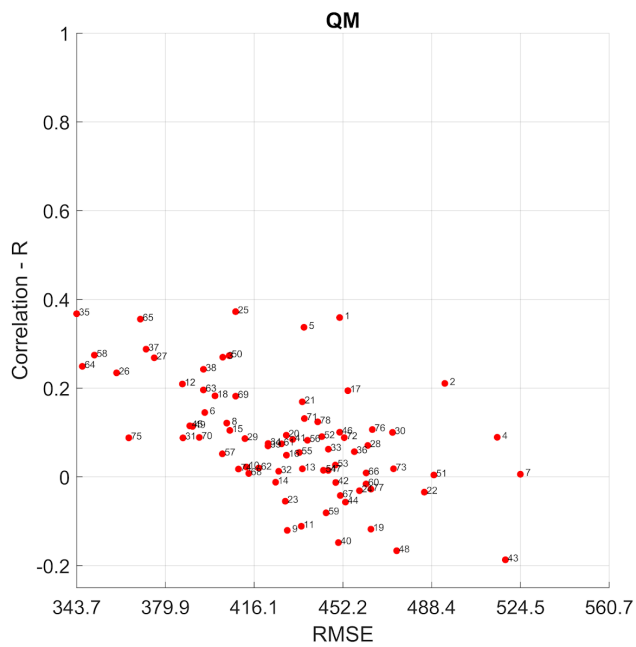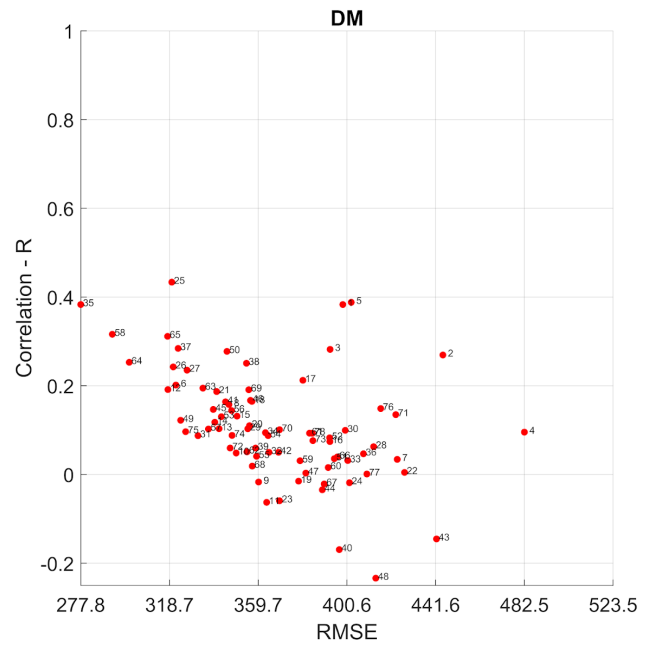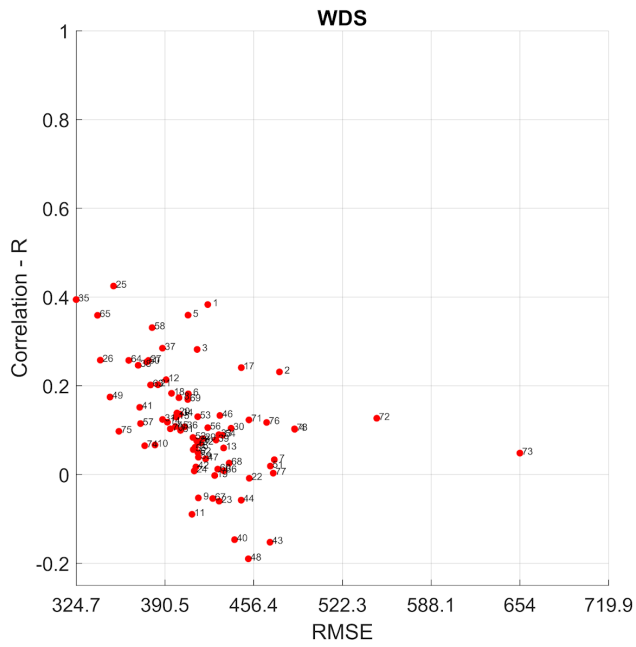
Figure 4 Median performance metrics (RMSE and R) for estimated total precipitation from series simulated by GCMs, without downscaling (WDS), as well as adjusted series obtained using the DM, QM, and RT.
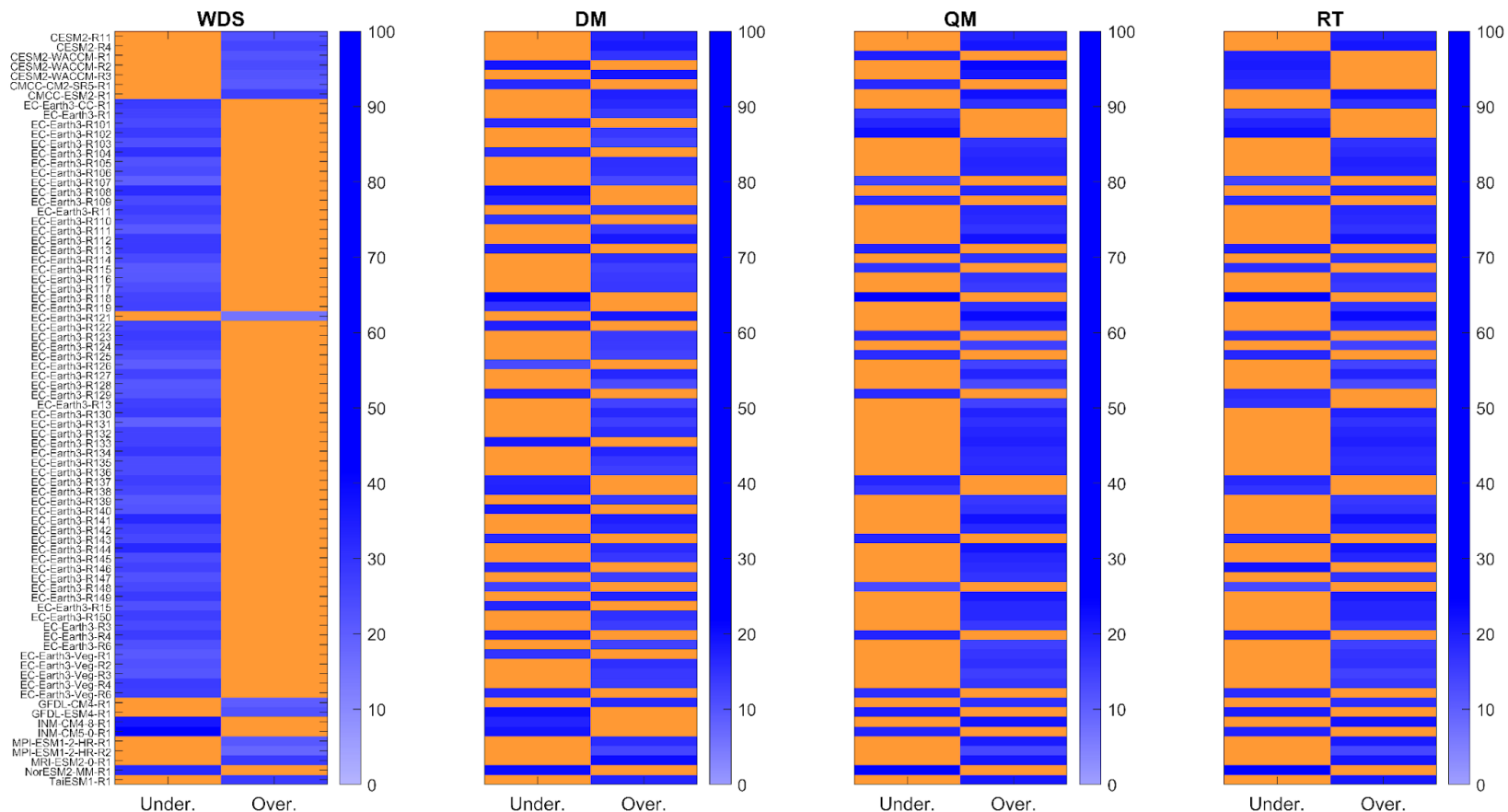
Figure 5 Median percentage error of underestimation or overestimation of total precipitation per hydrological year. The percentage error of the prevailing condition of underestimation (Under.) or overestimation (Over.) is represented in blue, while the non-prevailing condition is depicted in orange. For example, if underestimation is prevalent, overestimation is represented in orange. WDS represents the condition without the application of downscaling techniques, DM corresponds to the condition when the Delta Method is applied, QM represents the condition when Quantile Mapping is applied, and RT indicates the condition of applying Regression Trees as a downscaling technique.

3.2 Total precipitation and number of rainy days at multiyear level.

In the multiyear context, estimates derived from downscaled series using DM, QM, and RT showed more robust agreement with the estimations made from the historical records compared to the annual scale. A low discrepancy between the number of rainy days and total precipitation was observed at the multiyear scale.

When examining the number of rainy days, it was noted that the smallest errors are achieved when employing QM and RT as downscaling techniques. Additionally, estimates derived from downscaled series through DM demonstrated a performance similar to cases where no downscaling technique was applied (see Figure 6 and Table 4). Thus, in the multiyear scale, the series adjusted by QM yielded the smallest percentage errors, followed by those adjusted by RT and DM.

Table 4 Summary of percentual errors of number of rainy days in the multiyear level.

	SDS	DM	QM	RT
Maximum	141.90%	116.78%	1.21%	2.58%
Median	83.90%	77.88%	0.60%	1.83%
minimum	21.56%	1.20%	0.27%	1.19%

On the other hand, it was observed that the estimation of total precipitation at the multiyear scale, from series downscaled by DM, QM, and RT, significantly reduces percentage errors compared to cases where no downscaling technique is applied (See Figure 7 and Table 5).

Table 5 Summary of percentual errors of total precipitation in the multiyear level.

	SDS	DM	QM	RT
Maximum	33.59%	1.55%	1.99%	1.83
Median	12.13%	0.81%	1.02%	0.89
minimum	7.62%	0.43%	0.00%	0.01

Based on the results, employing downscaled series for estimating total precipitation and the number of rainy days on a hydrological year scale demonstrates better performance in the multi-year context. Therefore, it is recommended to utilize downscaled series by employing DM, QM, and RT for estimating total precipitation and the number of rainy days at the multi-year scale.

It was observed that the performance of downscaling techniques at the annual scale was consistently reflected at the multiyear scale. Regarding the number of rainy days, the QM method demonstrated superior performance across both annual and multiyear scales. As for total precipitation per hydrological year, the DM method showcased the best performance, exhibiting even higher efficiency at the multiyear scale.
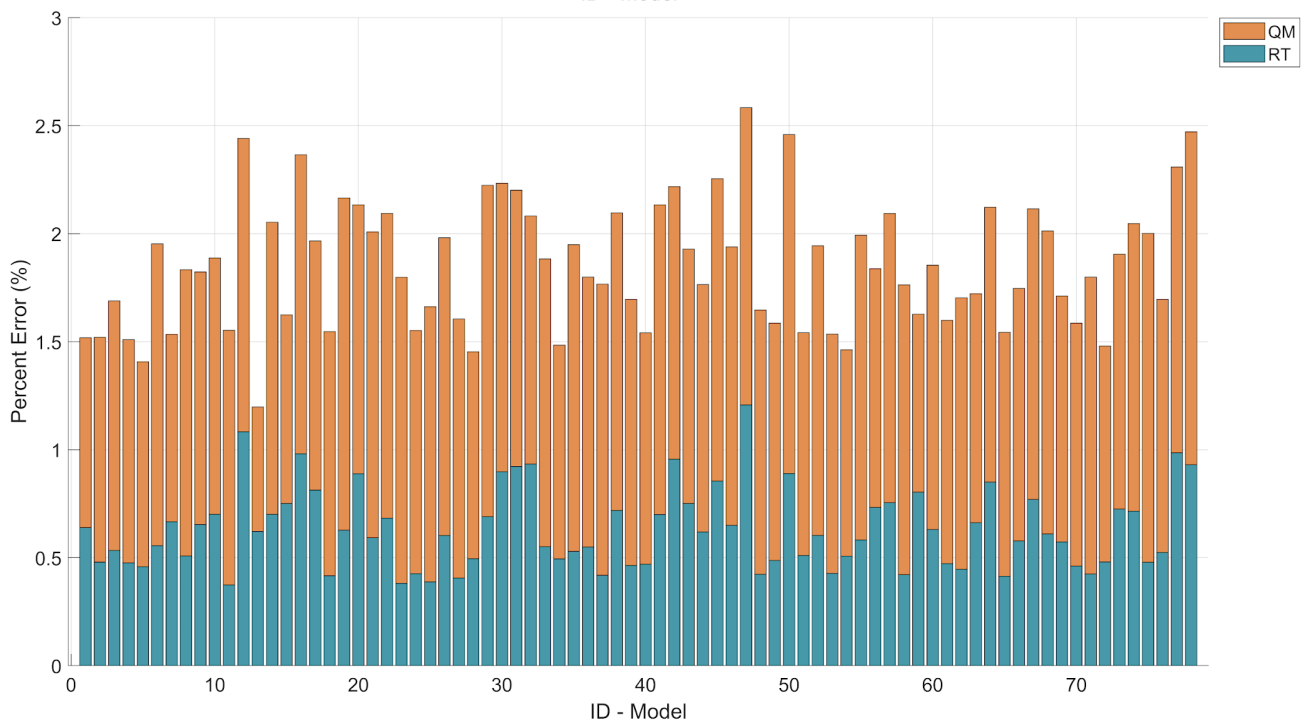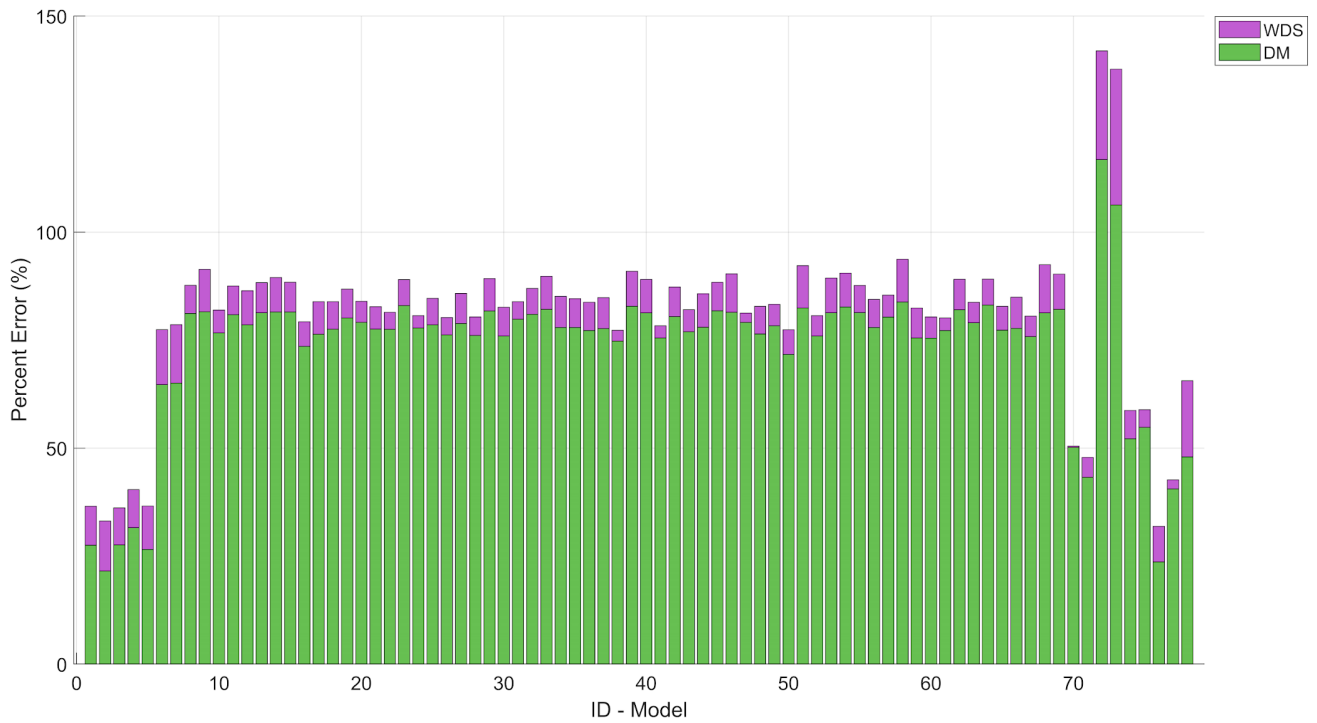
316
317 Figure 6 Median of Percentage Errors of Rainy Days at the multiyear level to each model. Without the application of
318 downscaling techniques (WDS), and with the application of Delta Method (DM), Quantile Mapping (QM), and Regression
319 Trees (RT) as downscaling techniques.

320

321

Figure 7 Median of Percentage Errors of total precipitation at the multiyear level to each model. Without the application of downscaling techniques - WDS, and with the application of Delta Method - DM, Quantile Mapping - QM, and Regression Trees - RT as downscaling techniques.

3.1 Frequency Analysis

Developed frequency analyses from downscaled series using QM and RT yield satisfactory results, evidenced by good performance in the NSE and KGE metrics. With respect to the frequency analyses developed from series downscaled by the DM method, it is observed that the results were comparable to those obtained when no downscaling technique was applied (see Figure 8 and Table 6).

Figure 8 illustrates a significant improvement in yield metrics following the implementation of QM and RT. The metrics approach unity, suggesting that the quantiles estimated from the adjusted series closely align with those derived from the historical series.

The percentage errors obtained in the estimates made with series downscaled by QM and RT were less than 12.18% and 5.91%, respectively. In contrast, the errors in the estimates made with series downscaled by the DM method were similar to those obtained when no downscaling technique was applied (See Table 6).

Table 6 Summary of percentual errors obtained in the Frequency analysis.

	SDS	DM	QM	RT
Maximum	57.95%	55.9%	12.18%	5.91%
Median	52.69%	47.1%	7.38%	1.56%
minimum	1.97%	0.45%	1.21%	0.09%

The high performance achieved in the estimation of quantiles from adjusted series through QM and RT is associated with the fact that the largest quantiles simulated by GCMs are correlated with the largest observed quantiles. Consequently, observed and simulated series of maximum values end up close values. This fact leads to comparable outcomes in estimations, regardless of whether they are derived from observed or downscaled series.

Given that downscaling in the case of DM is accomplished through the application of factors, the difference between the maximum precipitation observed and estimated from the adjusted series is substantial. Consequently, this results in a significant disparity in the outcomes of frequency analysis.

It was evident that the dispersion and variability of estimated quantiles from the adjusted series increased as the return period extended; however, this must be associated with the low occurrence of quantiles with high return times in the historical series (See Figure 10). Additionally, it was observed that errors related to DM are associated with an underestimation of quantiles for different return periods. Thus, it is concluded that the development of frequency analyses from adjusted series through QM and RT is feasible, with RT emerging as the technique that exhibited the best performance.
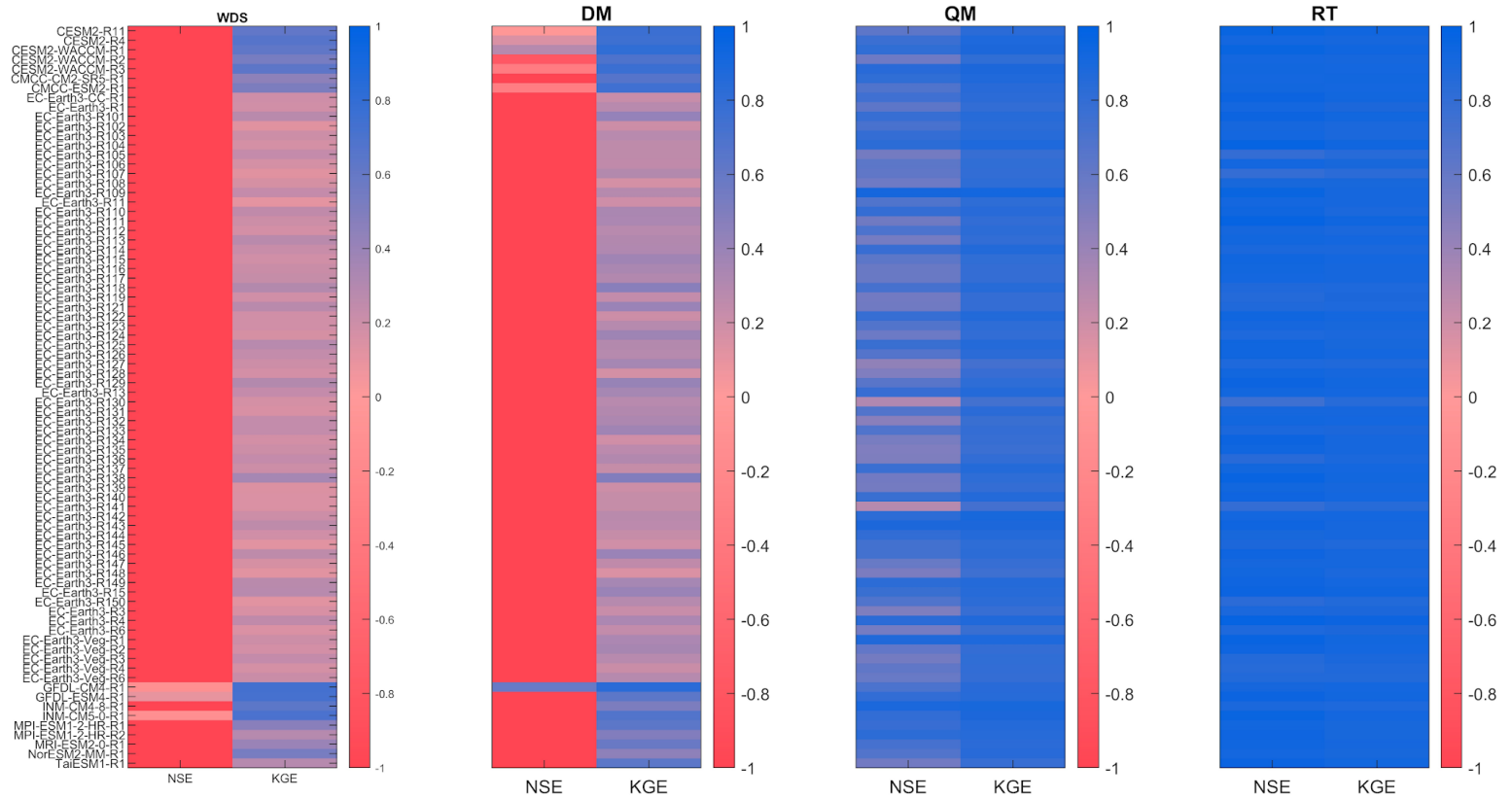
Figure 8 Median performance metrics (NSE e KGE) for the frequency analysis developed from precipitation series simulated by GCMs, without the application of downscaling techniques (WDS), as well as adjusted series obtained using the Delta Method (DM), Quantile Mapping (QM), and Regression Trees (RT).
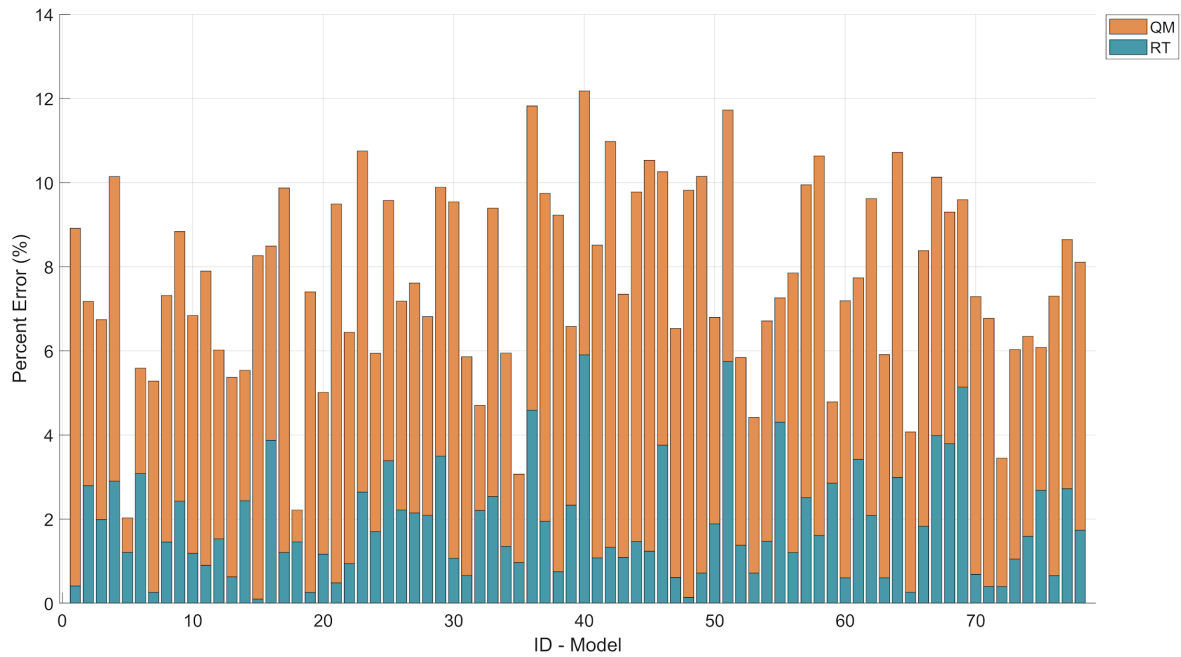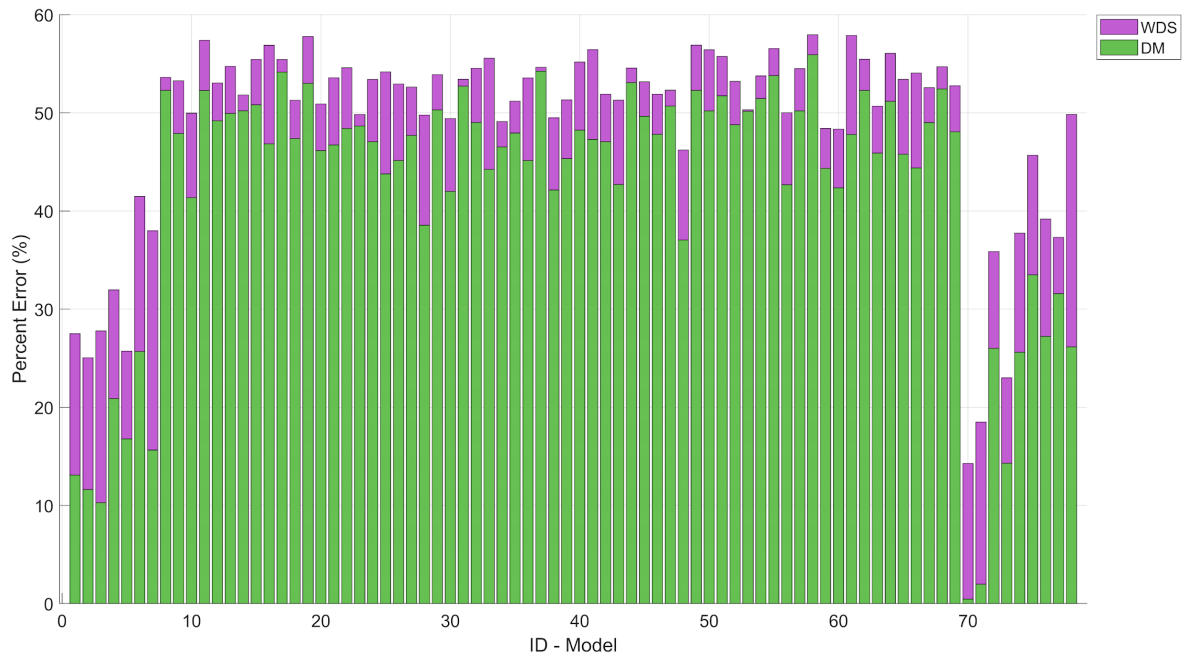
Figure 9 Median of percentual error obtained in the frequency analysis developed from precipitation series simulated by GCMs, without the application of downscaling techniques WDS, as well as reduced series obtained using the Delta Method - DM, Quantile Mapping - QM, and Regression Trees - RT.
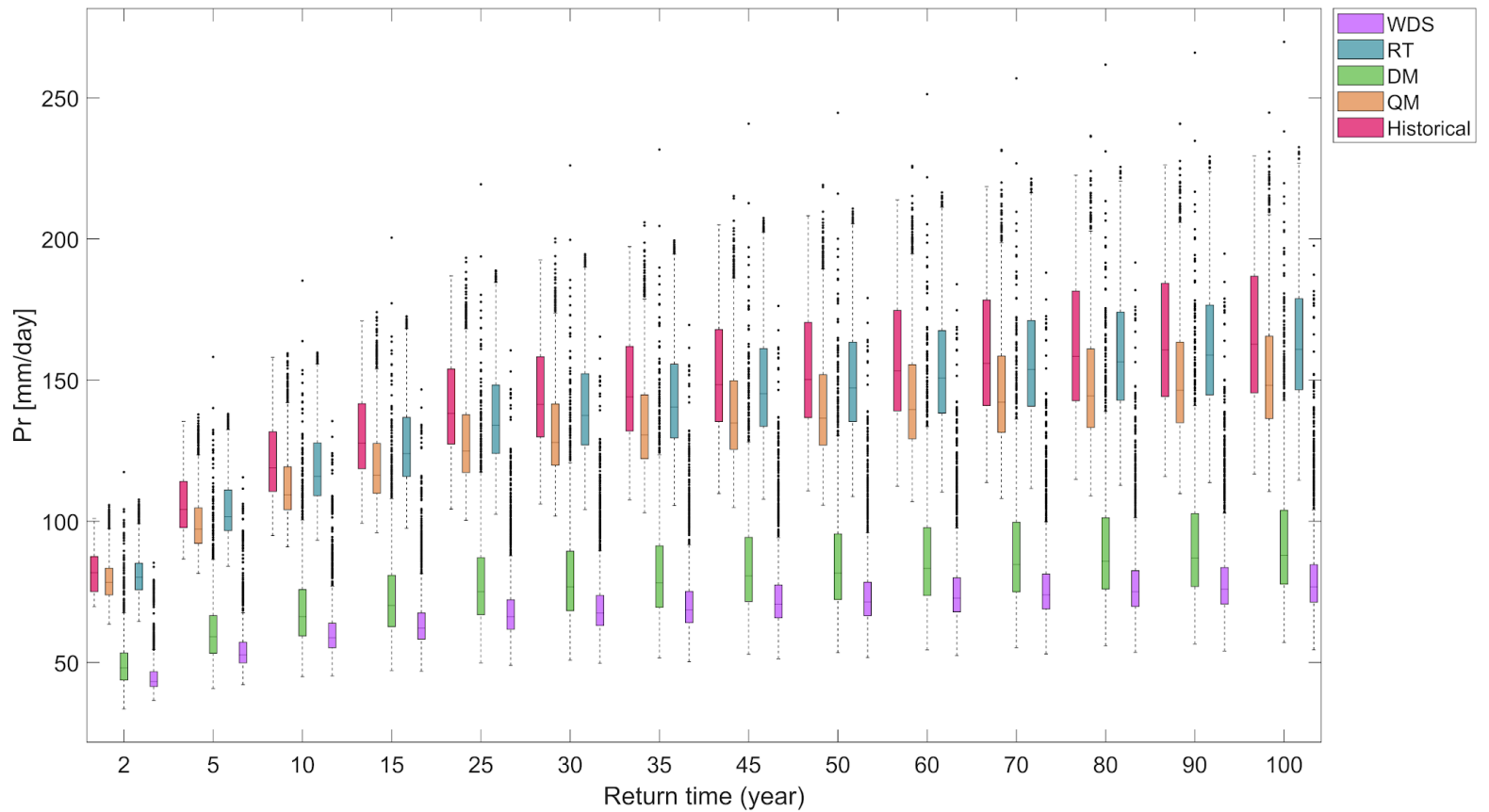
360
361 Figure 10 Frequency analysis developed from precipitation series simulated by GCMs, without the application of downscaling techniques (WDS),
362 as well as adjusted series obtained using the Delta Method (DM), Quantile Mapping (QM), and Regression Trees (RT) for the return time of 2, 5,
363 10, 15, 25, 30, 35, 45, 50, 60, 70, 80, 90 and 100 years.

4. Conclusions

This study aimed to assess the performance of using downscaled series through the Delta Method, Quantile Mapping, and Regression Trees to develop frequency analysis and estimate total precipitation and the number of rainy days per hydrological year at annual and multiyear levels.

It was observed that the Global Climate Models (GCMs) from the sixth phase of the Coupled Model Intercomparison Project (CMIP6) underestimated the number of rainy days per hydrological year for MRBH, with a median of 78 days. When estimating the number of rainy days from the downscaled series by DM, the tendency of underestimation persists and insignificantly decreases to 73 days. It was also observed that, when employing downscaled series through the application of QM and RT, underestimation is reversed to a slight overestimation. The average overestimations were 18 days for QM and 19 days for RT. Despite the relatively low magnitude of overestimations, the low NSE and KGE scores suggest that estimating the number of rainy days at an annual scale from downscaled series using DM, QM, and RT does not guarantee accurate results.

Similarly, GCMs underestimate total precipitation for the hydrological year, with a median of 413.84 mm. The use of a downscaled series by the DM reduces this difference to 361.42 mm. However, when QM and RT are applied, the differences surpass those without downscaling. The median differences in those cases are 433.10 mm for QM and 434.64 mm for RT. These facts, along with the low NSE and KGE scores, suggest that annual estimations of the number of rainy days and total precipitation from downscaled series by DM, QM, and RT do not yield reliable results. This result is also due to the fact that a one-year time window is not optimal for analysing the precipitation simulated by the considered RCMs, and consequently, more significant results were found with the multiyear study.

Therefore, at the multiyear scale, the estimation of the number of rainy days and total precipitation demonstrated high performance. For the number of rainy days, the percentage errors between the magnitudes of the total estimated from adjusted and observed series were less than 1.21% and 2.58% when downscaled series by QM and RT were employed. Percentage errors for estimating total rainfall per hydrological year on a multiyear scale were 1.55%, 1.99%, and 1.83% when downscaled series by DM, QM, and RT were used, respectively.

Finally, developing frequency analysis from the daily precipitation simulated by the MCGs allows obtaining quantiles close to those estimated with historical records when QM and RT are applied. The performance achieved in estimating quantiles from adjusted series by QM and RT is attributed to the fact that QM and RT associate the largest quantiles simulated by GCMs with the largest observed quantiles. As a result, observed and downscaled series have close values. The percentage error of estimates made from downscaled series by QM and RT, in relation to estimates based on observed data, were lower than

393   12.18% and 5.91%, respectively. In this context, it is recommended to utilize downscaling based on RT when the goal is to

394   assess future changes in frequency of occurrence.

395   **References**

396

397   Fadhel, S., Rico-Ramirez, M. A., & Han, D. (2017). Uncertainty of Intensity–Duration–Frequency (IDF) curves due to varied

398   climate baseline periods. *Journal of Hydrology*, *547*, 600–612. https://doi.org/10.1016/j.jhydrol.2017.02.013

399   Ghasemi Tousi, E., O'Brien, W., Doulabian, S., & Shadmehri Toosi, A. (2021). Climate changes impact on stormwater

400   infrastructure design in Tucson Arizona. *Sustainable Cities and Society*, *72*, 103014.

401   https://doi.org/10.1016/j.scs.2021.103014

402   Gupta, H. V., Kling, H., Yilmaz, K. K., & Martinez, G. F. (2009). Decomposition of the mean squared error and NSE

403   performance criteria: Implications for improving hydrological modelling. *Journal of Hydrology*, *377*(1–2), 80–91.

404   https://doi.org/10.1016/j.jhydrol.2009.08.003

405   Hashmi, M. Z., Shamseldin, A. Y., & Melville, B. W. (2011). Statistical downscaling of watershed precipitation using Gene

406   Expression Programming (GEP). *Environmental Modelling & Software*, *26*(12), 1639–1646.

407   https://doi.org/10.1016/j.envsoft.2011.07.007

408   Hassanzadeh, E., Nazemi, A., & Elshorbagy, A. (2014). Quantile-Based Downscaling of Precipitation Using Genetic

409   Programming: Application to IDF Curves in Saskatoon. *Journal of Hydrologic Engineering*, *19*(5), 943–955.

410   https://doi.org/10.1061/(ASCE)HE.1943-5584.0000854

411   Heo, J.-H., Ahn, H., Shin, J.-Y., Kjeldsen, T. R., & Jeong, C. (2019). Probability Distributions for a Quantile Mapping

412   Technique for a Bias Correction of Precipitation Data: A Case Study to Precipitation Data Under Climate Change.

413   *Water*, *11*(7), 1475. https://doi.org/10.3390/w11071475

414   Hutengs, C., & Vohland, M. (2016). Downscaling land surface temperatures at regional scales with random forest regression.

415   *Remote Sensing of Environment*, *178*, 127–141. https://doi.org/10.1016/j.rse.2016.03.006

416 IPCC, I. P. on C. C. (2014). *Climate Change 2014 Mitigation of Climate Change: Working Group III Contribution to the Fifth*

417 *Assessment Report of the Intergovernmental Panel on Climate Change*.

418 https://www.ipcc.ch/site/assets/uploads/2018/02/ipcc_wg3_ar5_frontmatter.pdf

419 Jakob Themeßl, M., Gobiet, A., & Leuprecht, A. (2011). Empirical-statistical downscaling and error correction of daily

420 precipitation from regional climate models. *International Journal of Climatology*, *31*(10), 1530–1544.

421 https://doi.org/10.1002/joc.2168

422 Jimenez, D. A. (2022). *Avaliação das alterações nas frequências de ocorrência das precipitações diárias máximas para a*

423 *região Metropolitana de Belo Horizonte considerando diferentes cenários de climas futuros.* [Universidade Federal

424 de Minas Gerais - UFMG]. https://repositorio.ufmg.br/handle/1843/46268

425 Khalid, I. A., & Sitanggang, I. S. (2022). *Machine Learning-Based Spatial Downscaling on Precipitation Satellite Data in*

426 *Riau Province, Indonesia*. 10.

427 Kreienkamp, F., Paxian, A., Früh, B., Lorenz, P., & Matulla, C. (2019). Evaluation of the empirical–statistical downscaling

428 method EPISODES. *Climate Dynamics*, *52*(1), 991–1026. https://doi.org/10.1007/s00382-018-4276-2

429 Liu, W., Bailey, R. T., Andersen, H. E., Jeppesen, E., Nielsen, A., Peng, K., Molina-Navarro, E., Park, S., Thodsen, H., &

430 Trolle, D. (2020). Quantifying the effects of climate change on hydrological regime and stream biota in a

431 groundwater-dominated catchment: A modelling approach combining SWAT-MODFLOW with flow-biota empirical

432 models. *Science of The Total Environment*, *745*, 140933. https://doi.org/10.1016/j.scitotenv.2020.140933

433 Loh, W. (2011). Classification and regression trees. *WIREs Data Mining and Knowledge Discovery*, *1*(1), 14–23.

434 https://doi.org/10.1002/widm.8

435 Mahla, P., Lohani, A. K., Chandola, V. K., Thakur, A., Mishra, C. D., & Singh, A. (2019). Downscaling Of Precipitation Using

436 Statistical Downscaling Model and Multiple Linear Regression Over Rajasthan State. *Current World Environment*,

437 *14*(1), 68–98. https://doi.org/10.12944/CWE.14.1.09

438 Mann, H. B., & Whitney, D. R. (1947). On the test of wheter one of random variables is stochastically larger than the other.

439 *Annals of Mathematical Statistics*.

440 Naghettini, M., & Pinto, É. J. (2007). *Hidrologia Estatística*. CPRM.

441   Nash, J. E., & Sutcliffe, J. V. (1979). *River flow forecasting through conceptual models part I — A discussion of principles—*

442   *ScienceDirect*. https://doi.org/10.1016/0022-1694(70)90255-6

443   NERC, N. E. R. C. (1975). *Flood Studies Report*.

444   Norris, J., Chen, G., & Li, C. (2020). Dynamic Amplification of Subtropical Extreme Precipitation in a Warming Climate.

445   *Geophysical Research Letters*, *47*(14). https://doi.org/10.1029/2020GL087200

446   Olsson, J., Arheimer, B., Borris, M., Donnelly, C., Foster, K., Nikulin, G., Persson, M., Perttu, A.-M., Uvo, C., Viklander, M.,

447   & Yang, W. (2016). Hydrological Climate Change Impact Assessment at Small and Large Scales: Key Messages

448   from Recent Progress in Sweden. *Climate*, *4*(3), 39. https://doi.org/10.3390/cli4030039

449   Onyutha, C., Tabari, H., Rutkowska, A., Nyeko-Ogiramoi, P., & Willems, P. (2016). Comparison of different statistical

450   downscaling methods for climate change rainfall projections over the Lake Victoria basin considering CMIP3 and

451   CMIP5. *Journal of Hydro-environment Research*, *12*, 31–45. https://doi.org/10.1016/j.jher.2016.03.001

452   Ostad-Ali-Askari, K., Ghorbanizadeh Kharazi, H., Shayannejad, M., & Zareian, M. J. (2020). Effect of Climate Change on

453   Precipitation Patterns in an Arid Region Using GCM Models: Case Study of Isfahan-Borkhar Plain. *Natural Hazards*

454   *Review*, *21*(2), 04020006. https://doi.org/10.1061/(ASCE)NH.1527-6996.0000367

455   Ozbuldu, M., & Irvem, A. (2021). Evaluating the effect of the statistical downscaling method on monthly precipitation

456   estimates of global climate models. *Global NEST Journal*, *23*(2), 232–240. https://doi.org/10.30955/gnj.003458

457   Rastogi, D., Kao, S.-C., & Ashfaq, M. (2022). How May the Choice of Downscaling Techniques and Meteorological Reference

458   Observations Affect Future Hydroclimate Projections? *Earth's Future*, *10*(8), e2022EF002734.

459   https://doi.org/10.1029/2022EF002734

460   Riahi, K., van Vuuren, D. P., Kriegler, E., Edmonds, J., O'Neill, B. C., Fujimori, S., Bauer, N., Calvin, K., Dellink, R., Fricko,

461   O., Lutz, W., Popp, A., Cuaresma, J. C., Kc, S., Leimbach, M., Jiang, L., Kram, T., Rao, S., Emmerling, J., … Tavoni,

462   M. (2016). The Shared Socioeconomic Pathways and their energy, land use, and greenhouse gas emissions

463   implications: An overview. *Global Environmental Change*, *42*, 153–168.

464   https://doi.org/10.1016/j.gloenvcha.2016.05.009

Roca, V., B., Beltrán, S. M., & Gómez, H. R. (2019). Cambio climático y salud. *Revista Clínica Española*, *219*(5), 260–265. https://doi.org/10.1016/j.rce.2019.01.004

Sachindra, D. A., Ahmed, K., Rashid, Md. M., Shahid, S., & Perera, B. J. C. (2018). Statistical downscaling of precipitation using machine learning techniques. *Atmospheric Research*, *212*, 240–258. https://doi.org/10.1016/j.atmosres.2018.05.022

Sachindra, D. A., Ahmed, K., Shahid, S., & Perera, B. J. C. (2018). Cautionary note on the use of genetic programming in statistical downscaling. *International Journal of Climatology*, *38*(8), 3449–3465. https://doi.org/10.1002/joc.5508

Salehnia, N., Hosseini, F., Farid, A., Kolsoumi, S., Zarrin, A., & Hasheminia, M. (2019). Comparing the Performance of Dynamical and Statistical Downscaling on Historical Run Precipitation Data over a Semi-Arid Region. *Asia-Pacific Journal of Atmospheric Sciences*, *55*(4), 737–749. https://doi.org/10.1007/s13143-019-00112-1

Salehnia, N., Salehnia, N., Saradari Torshizi, A., & Kolsoumi, S. (2020). Rainfed wheat (Triticum aestivum L.) yield prediction using economical, meteorological, and drought indicators through pooled panel data and statistical downscaling. *Ecological Indicators*, *111*, 105991. https://doi.org/10.1016/j.ecolind.2019.105991

Shahabul Alam, Md., & Elshorbagy, A. (2015). Quantification of the climate change-induced variations in Intensity–Duration–Frequency curves in the Canadian Prairies. *Journal of Hydrology*, *527*, 990–1005. https://doi.org/10.1016/j.jhydrol.2015.05.059

Tabari, H., Paz, S. M., Buekenhout, D., & Willems, P. (2021). Comparison of statistical downscaling methods for climate change impact analysis on precipitation-driven drought. *Hydrology and Earth System Sciences*, *25*(6), 3493–3517. https://doi.org/10.5194/hess-25-3493-2021

Teutschbein, C., & Seibert, J. (2012). Bias correction of regional climate model simulations for hydrological climate-change impact studies: Review and evaluation of different methods. *Journal of Hydrology*, *456–457*, 12–29. https://doi.org/10.1016/j.jhydrol.2012.05.052

Teutschbein, C., Wetterhall, F., & Seibert, J. (2011). Evaluation of different downscaling techniques for hydrological climate-change impact studies at the catchment scale. *Climate Dynamics*, *37*(9–10), 2087–2105. https://doi.org/10.1007/s00382-010-0979-8

490 Waters, D., Watt, W. E., Marsalek, J., & Anderson, B. C. (2003). Adaptation of a Storm Drainage System to Accommodate

491 Increased Rainfall Resulting from Climate Change. *Journal of Environmental Planning and Management*, *46*(5),

492 755–770. https://doi.org/10.1080/0964056032000138472

493 Worku, G., Teferi, E., Bantider, A., & Dile, Y. T. (2021). Modelling hydrological processes under climate change scenarios

494 in the Jemma sub-basin of upper Blue Nile Basin, Ethiopia. *Climate Risk Management*, *31*, 100272.

495 https://doi.org/10.1016/j.crm.2021.100272

496 Yang, Y., Tang, J., Xiong, Z., Wang, S., & Yuan, J. (2019). An intercomparison of multiple statistical downscaling methods

497 for daily precipitation and temperature over China: Present climate evaluations. *Climate Dynamics*, *53*(7), 4629–

498 4649. https://doi.org/10.1007/s00382-019-04809-x

499 Zhang, Z., & Li, J. (2020). Big climate data. Em *Big Data Mining for Climate Change* (p. 1–18). Elsevier.

500 https://doi.org/10.1016/B978-0-12-818703-6.00006-4